eJNDT e-Journal of Nondestructive Testing - ISSN 1435-4934 - www.ndt.net

EWSHM 2024
11th European Workshop on Structural Health Monitoring

Convolutional autoencoder-based framework for damage localization under variable temperature

Rafael JUNGES [1], Luca LOMAZZI [1], Francesco CADINI [1], Marco GIGLIO [1]
[1] Politecnico di Milano, Milan, Italy, info-dmec@polimi.it

Abstract. Confounding factors such as variable temperature have an impact on Lamb wave behaviour, affecting the accuracy of damage localization methods based on such waves. In this study, an innovative approach to Lamb wave prediction based on convolutional autoencoders (CAEs) is proposed and applied to an experimental dataset consisting of Lamb wave acquisitions on a Carbon Fiber Reinforced Polymer (CFRP) plate under varying temperatures.

Leveraging an experimental dataset of Lamb wave signals acquired from a CFRP plate at different temperatures, this research focuses on utilizing CAEs to enhance the accuracy and reliability of damage localization. This algorithm extracts critical features from Lamb wave data, effectively recognizing subtle wave properties variations, thus significantly improving the precision of damage localization. Two different architectures of CAEs were evaluated. One which uses the temperature value as a direct input into the latent space of the autoencoder, and another that does not process the temperature value. This analysis was performed to demonstrate the actual impact of the temperature information on prediction accuracy and, furthermore, the accuracy of the CAEs at predicting Lamb wave signals for temperatures outside of their training dataset.

The results obtained demonstrate that the inclusion of the temperature information into the autoencoder architecture not only increased its accuracy for temperatures within its training dataset but also increased its robustness with regards to temperature variations, displaying better performance at predicting Lamb wave signals for temperatures outside of its training dataset. The algorithm proposed here presents a way forward for increasing the robustness and reliability of damage localization methods based on Lamb waves.

Keywords: convolutional autoencoder, Lamb wave, damage localization.

Introduction

Several studies have demonstrated the effectiveness of Lamb wave propagation analysis in localizing damage on plate-like structures [1–5]. As the wave travels through the medium, alterations of the medium's properties, e.g., delamination or cracks on a plate, alter the wave speed, amplitude, among other properties. The comparison between a newly sensed wave to

Media and Publishing Partner
https://doi.org/10.58286/29684

the baseline signal which represents the wave for the healthy state of the plate can be used to detect, localize, and quantify damage on the plate.

However, the manner in which these waves change due to variations of the plate properties can often be very subtle and undiscernible, e.g., the damage is minute and far from the path between actuator and sensor. For this reason, innovative approaches mostly based on machine learning have been recently developed to highlight damage induced Lamb wave variations. For instance, [6] and [7] both explore the use of Lamb waves for structural damage detection and localization, with [6] focusing on the application of model-assisted convolutional and recurrent neural networks, and [7] using a data-driven approach with a specific 1D-CNN (Convolutional Neural Network) algorithm. In [8], autoencoders have been proved suitable for this purpose as well. This particular type of deep neural network takes the input signal through an encoder reducing its dimensionality similarly as the CNN studied in [7], and attempts to reconstruct the signal based on its low dimension representation through a decoder. It calibrates its weights and biases attempting to minimize the reconstruction error between input and output. If it is trained on signals acquired when the structure was healthy, it is capable of highlighting whenever it deviates from the healthy state based on higher reconstruction errors.

This method captures whatever changes might exist between its training inputs and the current inputs, but it is not capable of identifying what caused these changes. And according to different studies [9–11], Lamb waves are sensible to many different cofounding factors, such as temperature. Therefore, if an autoencoder is trained to reconstruct the healthy state signal of a particular wave at a certain temperature, if the temperature changes, this autoencoder might falsely indicate that the structure is damaged.

In [12], a damage localization framework based on autoencoders proved reasonably effective in detecting and distinguishing damage, even in the presence of temperature variations. However, its effectiveness was tested for temperatures within the dataset used by the autoencoders for training.

This study focuses on the effectiveness of autoencoders for damage localization including for temperatures which were not previously seen by the autoencoders. It proposes a solution which could render the method more robust against temperature variations.

An opensource dataset with data acquired from an array of piezoelectric transducers placed on a CFRP plate, with data gathered at different temperatures, has been used to train two autoencoder architectures: one which processes only the wave signal, another that has the temperature added as an input into its latent space. Both autoencoders have been tested for their capability at predicting the signal for temperatures outside of their training dataset.

This paper is organized according to the following structure: Section 1, Materials and Methods, where a description of both the dataset used and the implementation of the method are presented. Section 2, Results and Discussion, displays the outcomes of the application of the proposed method along with insights based on the results obtained. Lastly, Section 3, Conclusions, presents an overview of the study performed and its end results and conclusions.

1. Materials and Methods

Two CAE architectures were trained on a dataset of Lamb wave acquisitions for various temperatures, with the objective of assessing the influence of the temperature information on their signal prediction capabilities.

1.1 Dataset

Data was taken from an opensource repository [13] with wave data from a CFRP square plate of 500mm side, 2mm thickness, and stacking sequence [45/0/−45/90/−45/0/45/90] S. An

array of 12 piezoelectric transducers was attached to the plate and signals were acquired in a round-robin fashion, resulting in 66 signals for each acquisition. Wave frequencies spanned from 40kHz to 260kHz at 20kHz intervals (40kHz acquisitions were used in this study). Temperatures ranged from 20°C to 60°C at approximately 0.5°C intervals.

To verify the autoencoder's capability at generalizing signals from outside its training dataset, three different temperature arrangements were used for autoencoder training:

a) 20°C - 60°C.
b) 20°C - 40°C - 60°C.
c) 20°C - 30°C - 40°C - 50°C - 60°C.

This approach covers the practical case in which experimental data from specific temperatures is missing and assesses the autoencoders capability at generalizing its predictions.

1.2 Convolutional Autoencoder

Convolutional autoencoders get this name from two aspects of their construction, the convolution process and the autoencoder architecture. Convolution entails the scanning of the input signal e.g., an image or in this case a wave signal, using the so-called filters or kernels. These filters are designed to highlight particular aspects of the input and reduce its dimensionality.

The autoencoder is a deep neural network in which the input signal has its dimensionality reduced while being projected onto what is called the latent space. This process is called encoding and is performed by the encoder part of the architecture. This latent space representation is then used as input by the decoder to reconstruct the input signal. During this process, the reconstruction error i.e., the difference between the input and the output of the entire autoencoder, is minimized by adjusting the weights and biases of the filters in both the encoder and decoder. There can be many network layers in both, which are usually symmetric with regards to the latent space i.e., same number of layers with the same input and output dimensions. Both architectures in this study are symmetric.

The reconstruction error utilized for the optimization process was the root mean squared error (RMSE). As for the architecture of the autoencoders, as previously mentioned, the intent of the study is to assess the influence of temperature in the autoencoder's generalization capability. Therefore, two different architectures were evaluated (Figure 1). It is worth noting that, for the autoencoder that processes the temperature as an input, the latent space had five points, one being the temperature value while the other 4 were the results of the input signal encoding. Meanwhile, the autoencoder without the temperature input had only the four nodes from the signal encoding.

As for the optimization strategy, the ADAM optimizer with the following parameters was used:

- Learning rate = 0.0001.
- Beta 1 = 0.9.
- Beta 2 = 0.999.
- Epsilon = 1e-07.

For training purposes, noise was added to the original dataset signals, generating 1000 samples of the same signal with a signal-to-noise ratio of 20 dB [14]. These signals were then divided into training (80%), testing (10%) and validation (10%). One autoencoder was

trained for each signal i.e., each actuator-sensor path, resulting in 66 autoencoders. The difference between each temperature arrangement is the amount of data available for the autoencoder for training, being 2000, 3000 and 5000 signals for cases a, b, and c, respectively.

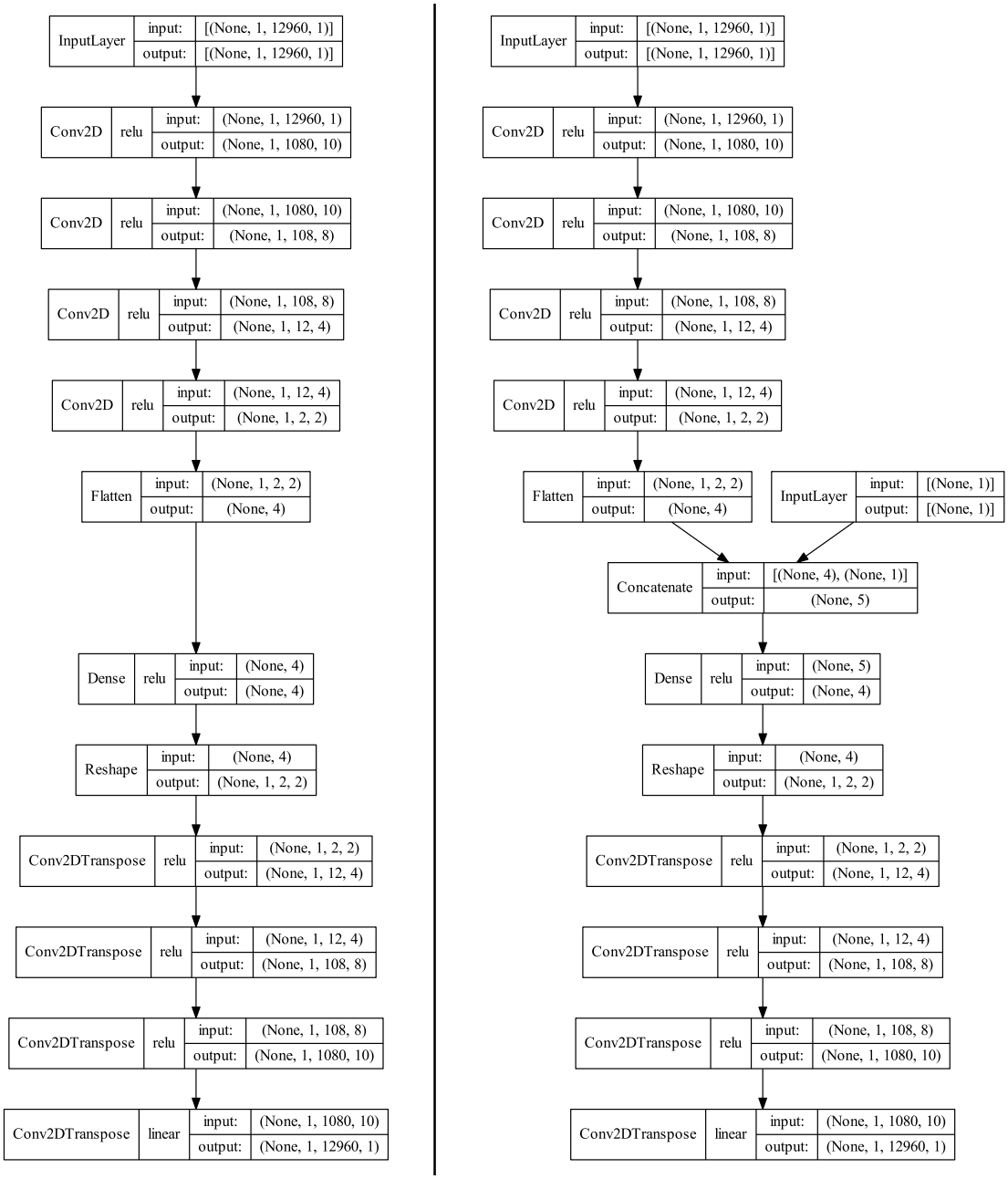

Fig. 1. Autoencoder architectures tested. On the right, the temperature is inserted directly into the latent space. On the left, only the signal is processed. The activation functions used by each layer are displayed along with the dimensions of its input and output.

2. Results and Discussion

Training performance with regards to training and validation loss was firstly analysed to ensure that the autoencoders were not underfitting or overfitting the training data. As can be seen in Figure 2, which displays the training performance of one illustrative CAE, training

was carried out without underfitting or overfitting, reaching training and validation losses below $1e^{-3}$.

Another measure of autoencoder adequacy is the comparison between the RMSE for healthy state signals i.e., the baseline, and damaged state signals, after autoencoder training. During the experimental campaign to generate the dataset used in this study, the researchers mounted aluminium discs on the surface of the specimen to simulate damage. If the RMSE for the healthy state signal is lower than the RMSE for the damaged state signal, the autoencoder can properly recognize possible damages. As can be seen in Figure 2, for the same CAE of the training performance plot, the RMSE for damaged state signals (200 in total, 100 for each temperature which in this case are 20°C and 60°C, taken from two original signals and adding 20dB signal-to-noise ratio) are higher than the RMSE for the healthy state signals, meaning that the autoencoders can be used for identifying damage.

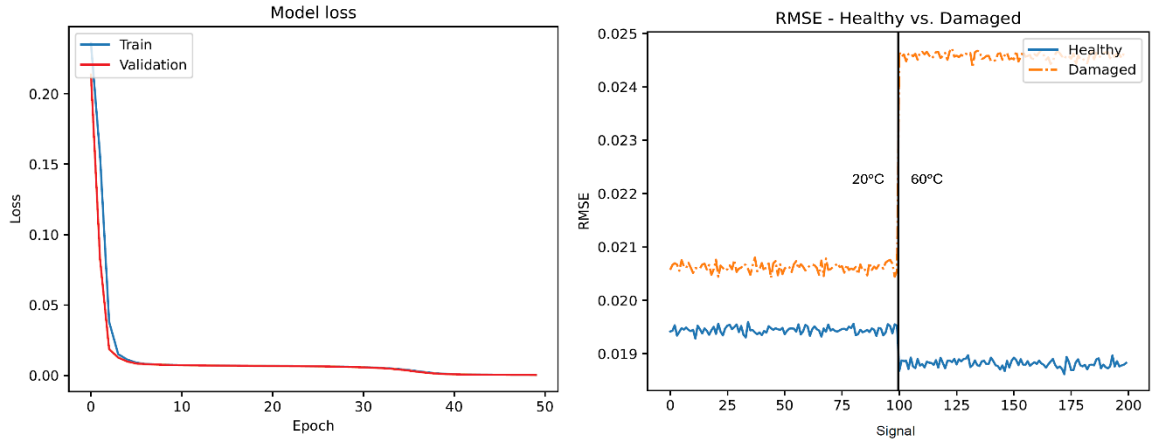

Fig. 2. Left: model loss during training for one of the autoencoders. Right: Reconstruction RMSE for the trained autoencoder, with damaged or healthy state signals as input.

The performance of the two different architectures at reconstructing healthy state signals was evaluated for the three different temperature arrangements for training described in Section 1.1, and the results can be seen in Figures 3, 4 and 5. The two different autoencoder architectures are represented with different colours, red being the CAE architecture with the temperature input. The RMSE results are grouped by temperature. Each box represents the 66 signals from each acquisition. The boxes extend from the 25th-percentile, meaning that 25% of the data is below that point, to the 75th-percentile, meaning that 75% of the data is below that point, with a line at the median. The whiskers extend to the farthest data point lying within 1.5 times the inter-quartile range from the box. Outliers are represented by circles.

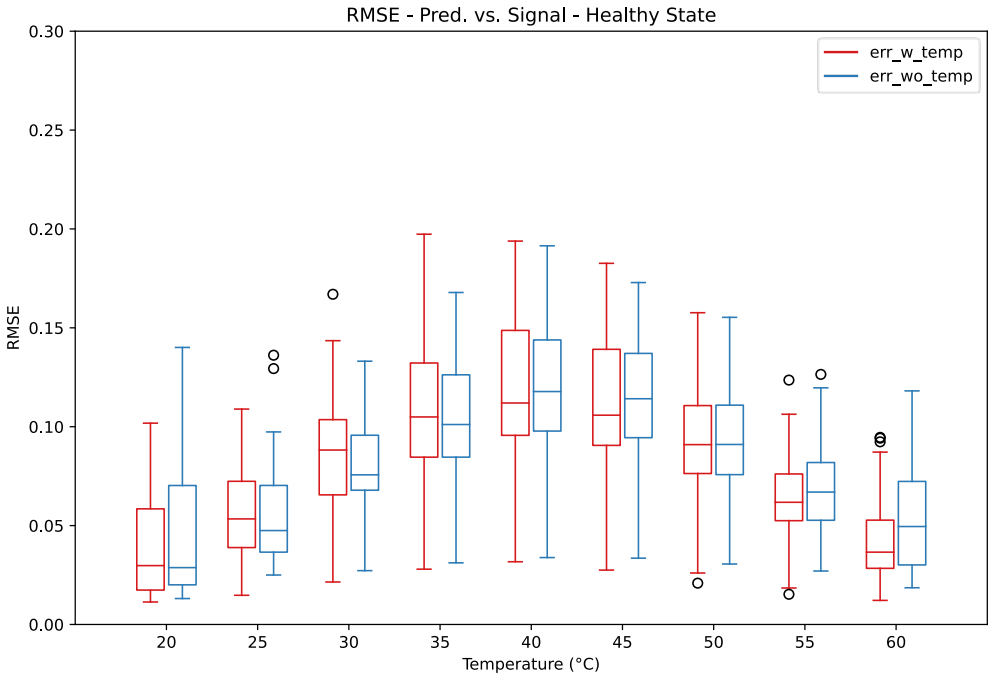

Fig. 3. Autoencoder performance with regards to reconstruction RMSE for all the actuator-sensor pairs, grouped by temperature. Training with 20°C and 60°C signals (case a).

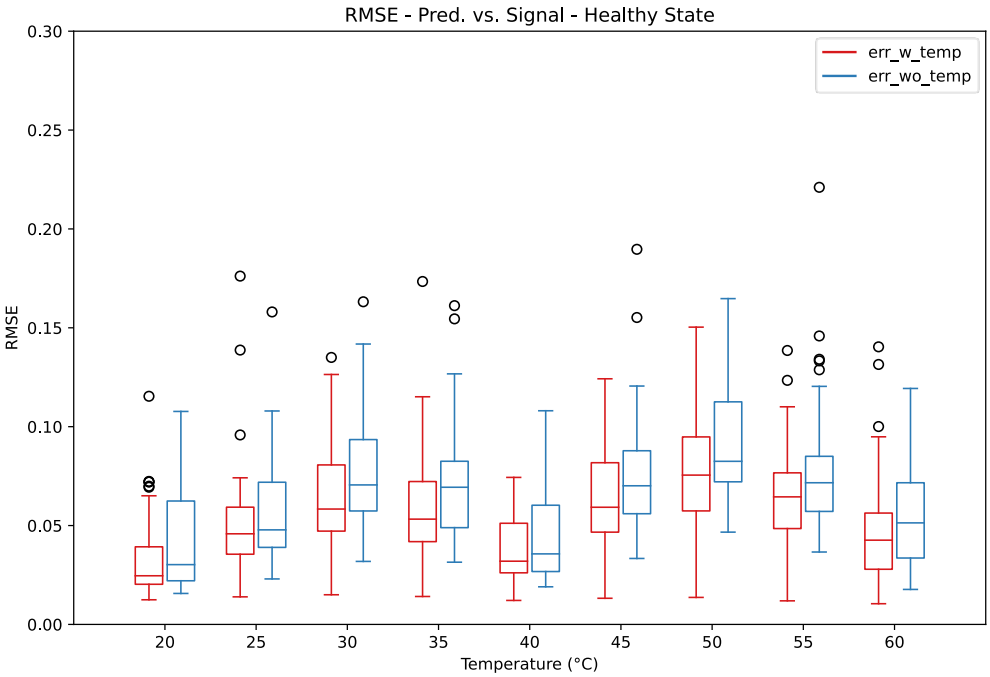

Fig. 4. Autoencoder performance with regards to reconstruction RMSE for all the actuator-sensor pairs, grouped by temperature. Training with 20°C, 40°C and 60°C signals (case b).

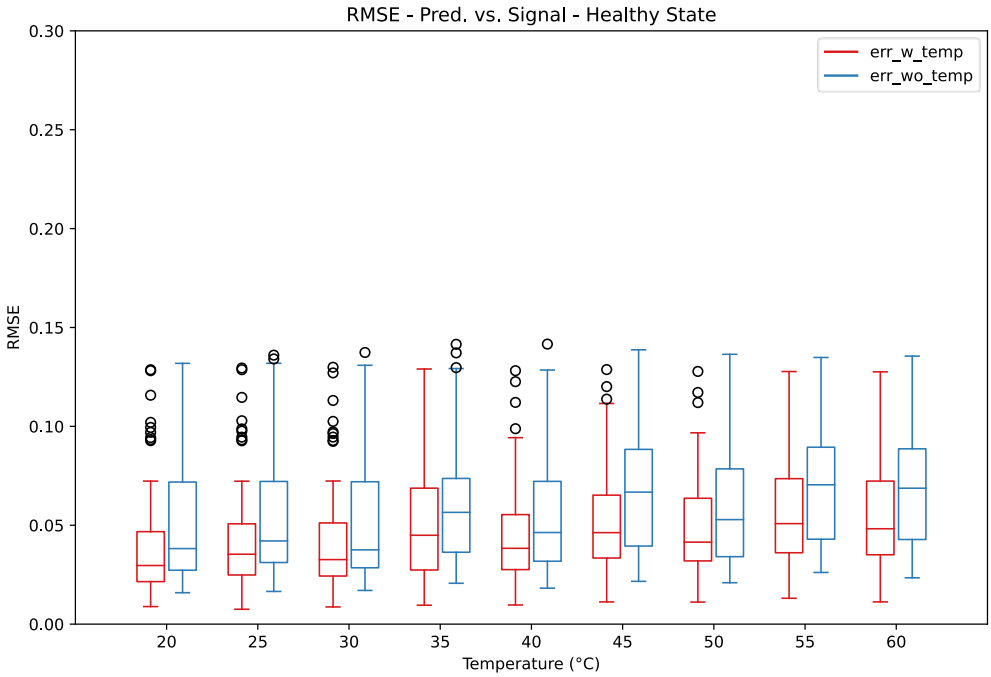

Fig. 5. Autoencoder performance with regards to reconstruction RMSE for all the actuator-sensor pairs, grouped by temperature. Training with 20°C, 30°C, 40°C, 50°C and 60° signals (case c).

By analysing the performance of both autoencoder architectures across various datasets some potentialities and drawbacks of the utilized algorithms can be highlighted.

The three plots demonstrate that for the temperatures included in the training of the CAEs, both architectures perform better than for temperatures outside of their training dataset, as expected. For case c, this difference is very much attenuated given the smaller temperature interval between training temperatures. Furthermore, it is noticeable that the RMSE keeps increasing for temperatures further away from the training temperatures, in a close to linear fashion.

Additionally, the architecture with the temperature performs consistently better at reconstructing the signals for all temperatures, even more for temperatures unseen by the autoencoders during training. Moreover, for case b, the autoencoder architecture with the embedded temperature was able to keep the minimum error at similar values across all temperatures. And for case a, for temperatures up to 35°C, the architecture without the temperature performed better, while for higher temperatures performance was slightly worse for both architectures.

3. Conclusion

For all training temperature arrangements, the CAE architecture with the temperature input performed better, therefore it is always advantageous to leverage this information within the autoencoder. For more sparse datasets, the benefit for including the temperature is slightly more noticeable.

If the dataset is too sparse and has just two temperature points for autoencoder training (case a), both architectures perform similarly, being unable to properly predict Lamb wave signals and displaying high RMSEs between input and output.

It is clear that a larger dataset with more temperature values for training increase the autoencoders performance, regardless of the architecture. But the architecture with the temperature input performs better all around, except for the lower temperatures in case a.

The method here proposed indicates a path towards more robust damage localization frameworks, able to predict healthy structure behaviour for untested temperatures and therefore recognizing damage for said temperatures. The results are still preliminary and damage localization results are still to be acquired in order to validate the results presented here. Nonetheless, the method seems promising and future work including damage localization using both architectures will be conducted.

Moreover, the influence of the temperature within the latent space can be further studied with regards to the size of the latent space. In the present study the temperature point represented 20% of the latent space, while the remaining 80% were points coming from the input signal encoding. Tests with different latent space configurations can further clarify the influence of the temperature point in the latent space.

References

[1] B. C. Lee and W. J. Staszewski, "Lamb wave propagation modelling for damage detection: I. Two-dimensional analysis," *Smart Mater Struct*, vol. 16, no. 2, p. 249, Jan. 2007, doi: 10.1088/0964-1726/16/2/003.

[2] A. Migot, Y. Bhuiyan, and V. Giurgiutiu, "Numerical and experimental investigation of damage severity estimation using Lamb wave–based imaging methods," *J Intell Mater Syst Struct*, vol. 30, no. 4, pp. 618–635, 2019, doi: 10.1177/1045389X18818775.

[3] Y. Wang, L. Qiu, Y. Luo, R. Ding, and F. Jiang, "A piezoelectric sensor network with shared signal transmission wires for structural health monitoring of aircraft smart skin," *Mech Syst Signal Process*, vol. 141, p. 106730, 2020, doi: https://doi.org/10.1016/j.ymssp.2020.106730.

[4] F. Gao, Y. Shao, J. Hua, L. Zeng, and J. Lin, "Enhanced wavefield imaging method for impact damage detection in composite laminates via laser-generated Lamb waves," *Measurement*, vol. 173, p. 108639, 2021, doi: https://doi.org/10.1016/j.measurement.2020.108639.

[5] G. Yan, "A Bayesian approach for damage localization in plate-like structures using Lamb waves," *Smart Mater Struct*, vol. 22, 2013, [Online]. Available: https://api.semanticscholar.org/CorpusID:137326476

[6] M. Rautela and S. Gopalakrishnan, "Lamb wave based structural damage detection and localization using model assisted convolutional and recurrent neural networks," *Expert Syst Appl*, vol. 167, p. 114189, 2021, doi: https://doi.org/10.1016/j.eswa.2020.114189.

[7] R. Cui, G. Azuara, F. L. di Scalea, and E. Barrera, "Damage imaging in skin-stringer composite aircraft panel by ultrasonic-guided waves using deep learning with convolutional neural network," *Struct Health Monit*, vol. 21, pp. 1123–1138, 2021, [Online]. Available: https://api.semanticscholar.org/CorpusID:236279219

[8] L. Lomazzi, R. Junges, M. Giglio, and F. Cadini, "Unsupervised data-driven method for damage localization using guided waves," *Mech Syst Signal Process*, vol. 208, p. 111038, 2024, doi: https://doi.org/10.1016/j.ymssp.2023.111038.

[9] J. Moll, C. Kexel, S. Pötzsch, M. Rennoch, and A. S. Herrmann, "Temperature affected guided wave propagation in a composite plate complementing the Open Guided Waves Platform," *Sci Data*, vol. 6, no. 1, p. 191, 2019, doi: 10.1038/s41597-019-0208-1.

[10] J. P. Andrews, A. N. Palazotto, M. P. DeSimio, and S. E. Olson, "Lamb Wave Propagation in Varying Isothermal Environments," *Struct Health Monit*, vol. 7, no. 3, pp. 265–270, 2008, doi: 10.1177/1475921708090564.

[11] R. Gorgin, Y. Luo, and Z. Wu, “Environmental and operational conditions effects on Lamb wave based structural health monitoring systems: A review,” *Ultrasonics*, vol. 105, p. 106114, 2020, doi: https://doi.org/10.1016/j.ultras.2020.106114.

[12] A. Abbassi, N. Römgens, F. F. Tritschel, N. Penner, and R. Rolfes, “Evaluation of machine learning techniques for structural health monitoring using Lamb waves under varying temperature conditions,” *Struct Health Monit*, vol. 22, no. 2, pp. 1308–1325, 2023, doi: 10.1177/14759217221107566.

[13] J. Moll, C. Kexel, S. Pötzsch, M. Rennoch, and A. S. Herrmann, “Temperature affected guided wave propagation in a composite plate complementing the Open Guided Waves Platform,” *Sci Data*, vol. 6, no. 1, p. 191, 2019, doi: 10.1038/s41597-019-0208-1.

[14] V. Ewald, R. M. Groves, and R. Benedictus, “DeepSHM: a deep learning approach for structural health monitoring based on guided Lamb wave technique,” in *Sensors and Smart Structures Technologies for Civil, Mechanical, and Aerospace Systems 2019*, J. P. Lynch, H. Huang, H. Sohn, and K.-W. Wang, Eds., SPIE, 2019, p. 109700H. doi: 10.1117/12.2506794.